Kinetik: Game Technology, Information System, Computer Network, Computing, Electronics, and Control
Journal homepage: http://kinetik.umm.ac.id
ISSN: 2503-2267
Vol. 7, No. 1, February, Pp. 81-90

EAM-LoRaNet: energy aware multi-hop LoRa network for internet of things

Misbahuddin*[1], Muhamad Syamsu Iqbal[2], Djul Fikry Budiman[3], Giri Wahyu Wiriasto[4], L. Ahmad S. Irfan Akbar[5]
University of Mataram, Mataram, Indonesia[1,2,3,4,5]

Article Info
Keywords:
Internet of Things, LPWAN, Energy-Aware, Multi-Hop LoRa, Network Lifetime

Article history:
Received: January 15, 2022
Accepted: February 07, 2022
Published: February 28, 2022

Cite:
M. Misbahuddin, M. S. . Iqbal, D. F. Budiman, G. W. . Wiriasto, and L. A. S. I. Akbar, "EAM-LoRaNet: Energy Aware Multi-hop LoRa Network for Internet of Things", *KINETIK*, vol. 7, no. 1, pp. 81-90, Feb. 2022.
https://doi.org/10.22219/kinetik.v7i1.1391

*Corresponding author.
Misbahuddin
E-mail address:
misbahuddin@unram.ac.id

Abstract
LoRa Technology is one of the devices used on Low-Power Wide Area Networks (LPWAN), which is a viable alternative wireless communication technology for the Internet of Things (IoT). The LoRa device is meant to traverse a large distance while using minimal power. However, because it uses single-hop communication, the Gateway's farthest nodes will die prematurely as a result of the increased energy usage. This research attempts to improve the range of LoRa networks utilizing multi-hop uplink communication while also reducing energy consumption by adjusting the LoRa transmission power to the lowest possible dBm in each hop. As a network model, a star topology-based tree made of some rings with a gateway as the central point is chosen. The performance of two forms of uplink communication, single-hop and multi-hop models was tested in terms of energy consumption and coverage. The results show that the network structure in the multi-hop uplink model can extend coverage over a greater distance while using less energy than the single-hop uplink model. This model can be used as a supplement to the LPWAN's uplink communication in the IoT to enhance the network's coverage range and lifetime.

1. Introduction

The Internet of things (IoT) communications in sensor node deployment for a variety of applications is predicted to increase rapidly and shortly. According to Ericsson [1], by 2025, Ericsson estimates that 5 billion IoT devices will be connected via cellular 3GPP access technologies. Furthermore, according to a Forbes survey, there will be roughly 75 billion IoT devices connected to the internet by 2025, and the exponential increase in IoT applications will affect all industrial processes and practically all market areas. To be more specific, it necessitates a rethinking of how to design, manage, and maintain connections, networks, big data, and the cloud.

The IoT uses two types of transmission to connect devices to the internet: local and internet connections. End devices collect and deliver sensed data and parameters to Gateway (GW) via radio connections in a local connection. Meanwhile, in the internet connection, the data is forwarded to an application server to be stored in the cloud. IoT local connections now use three types of wireless technologies, which are classified by range: short-range, medium-range, and long-range networks. For sensing applications in short-range networks, wireless technology such as RFID/NFC [2], Bluetooth Low Energy (BLE) [3], IEEE 802.15.6-based wireless body area networks [4], or IEEE 802.11a/b/g/n/ad/ac [5] can be employed. Furthermore, wireless devices such as IEEE 802.15.3-based wireless low-rate personal area networks [6] and IEEE 802.15.4 Zigbee [7] are employed in short-range situations for low data rate applications. On the other hand, cellular networks 5G [8] can be expanded to long-range networks, but they are designed for data and voice communication rather than wireless sensing applications. Long Range (LoRa) [9] [10], Sigfox [11], and NB-IoT [12] are some of the other device technologies that are suitable for wireless sensing applications in long-range applications.

Low Power Wide Area Networks (LPWAN), a new paradigm in IoT, use wireless technologies. This technology is being deployed and has shown tremendous promise for a wide range of IoT and M2M applications [13], particularly in constrained environments. In general, LPWAN is a sort of wireless IoT communication standard with low transmission data rates and small packet data sizes that can be used to expand coverage regions and improve battery life [14] [15]. As a result, LoRa technology, as one of the LPWAN devices, is a potential wireless IoT communication technology that is extensively employed since it can serve as an energy-efficient and low-complexity end device for a number of applications that are to be implemented on scalable networks. On the other hand, the LPWAN employs a star topology with end devices communicating directly with the gateway (GW). In the architecture of the routing protocol, this communication paradigm is referred to as a single-hop method. Furthermore, it establishes a reliable technique for network centralized control. However, because each end device is designed to link directly to the GW, the network relies significantly on the transceiver's capabilities in this manner. As a result, the single-battery-powered end devices that are farthest from the GW will experience early energy depletion, reducing the network lifetime. As a consequence, in order to extend the network's lifetime, energy consumption is a vital issue to consider.

Researchers have devised models to create numerous novel multi-hop protocols to extend the network lifetime and expand network coverage in the star LPWAN architecture. These protocols can be divided into two categories: (i) multi-hop protocol based on the LoRa, (ii) multi-hop routing using the existing LoRaWAN. The first work that introduces a multi-hop LoRa-based network was being called LoRaBlink [16]. This protocol works over LoRa physical layer integrating MAC and routing at the same layer. The multi-hop network is begun with time synchronization among nodes to create slotted channel access so that the nodes can transmit packets concurrently. The sink can distribute a packet to nodes using flooding, likewise, the nodes transmit a packet to the sink that employs directed flooding. The tests have shown a reliability of 80%. The concurrent transmission (CT) technique [17] also used a revolutionary flooding routing protocol that has been successfully implemented in IEEE 802.15.4-based networks. The CT protocol does not require a routing table, and the nodes are synchronized via the flooding process. The protocol improves LoRa coverage and delivers a dependable packet delivery rate in the specified indoor situation. The energy consumption is not examined but tested by several proof-of-concept studies that have shown that the concept works well indoors, especially when the nodes are nearly together.

The research in [18] presents a mesh network solution based on LoRa transceiver for dealing with poor packet delivery ratios (PDRs). The gateway, which periodically requests data from each of the linked nodes, has sole control over medium access. None of the nodes is permitted to transfer data actively. This approach prevents collisions, but it necessitates that each child node is in 'receive' mode at all times to ensure that all query requests are received. This research did not focus on either power consumption optimization or time synchronization. Another drawback is that the number of supported nodes is limited because each message is sent instantly rather than sending all incoming packets in a single packet to the next node on the way to the gateway.

In [19] it creates a lightweight LoRa protocol by combining the Hybrid Wireless Mesh Protocol (HWMP) and the Ad hoc On-Demand Distance Vector (AODV) protocol. This approach uses intermediate nano-gateways that do not fully support LoRaWAN, and the routing technique is transparent to end devices and the network server. Only route construction delays are included while evaluating the protocol. On the other hand, the Destination-Sequenced Distance Vector (DSDV) routing protocol was adapted for LoRaWAN by the developers of [20]. The proposed system divides nodes into two types: routing nodes and leaf nodes, with routing devices that are not limited by energy. The solution was put to the test in a prototype system in both linear and bottleneck scenarios. They conclude that the solution is viable, despite the duty cycle constraints.

A linear multi-hop LoRa [21] used a basic routing protocol and synchronization mechanism that uses a wake-up time transmission strategy to save energy. The results showed that the synchronization mechanism saves energy usage by 50% when compared to a non-optimal wake-up time. Moreover, a linear multi-hop network based on LoRa [22] was also investigated to extend the coverage area using a simple routing system. This protocol also incorporated a synchronization mechanism to the end devices and put the protocol into practice in a real-world setting. The testbed's throughput and reliability were used to evaluate its performance, rather than power consumption. Next, to increase the performance of the multi-hop LoRa networks, a network clustering based on the spreading factor established a tree-based SF clustering method (TSCA) that divides nodes into subnets [23]. Using numerous SFs, the author investigated the prospect of parallel transmission in LoRa. The authors used simulation and real-world scenarios to examine the solution and concluded that an efficient multi-hop LoRaWAN network must consider SF allocation.

The work given in [24] and [25] present a full protocol solution for the LoRa physical layer, which included TDMA access, collision avoidance, synchronization, and routing mechanisms to give a low latency solution. The results revealed that the protocol had good data dependability and minimal latency, but no information on energy consumption was provided.

The study in [26] presents a new LoRaWAN model to handle the challenge of underground infrastructure monitoring. The design consists of sensor nodes that create a LoRa mesh network and feed data to a repeater node that serves as a sensor sink. The repeater node is a small battery-powered end device that is not linked to the Internet that connects directly with the main gateway. In a mesh network, the sensor nodes act as routers, while the repeater node acts as a relay, forwarding messages to the gateway.

In this study, we propose a multi-hop LoRa-based network that provides a model for calculating the energy consumption of LPWAN. The model is also used for single-hop to compare the multi-hop network in terms of energy saving. The end devices in the network that cannot reach directly to the GW can forward their data to other end devices as an intermediate node in several hops. This mode has certainly a new problem in selecting an appropriate spreading factor to decrease energy consumption. Therefore, we introduce a new framework that is called Energy-Aware Multi-hop LoRa Network (EAM-LoRaNet) for a structure of the LPWAN that especially uses the LoRa device as the transceiver. This study aims to evaluate the performance of EAM-LoRaNet as a new alternative in a long-range transmission model of the LPWAN to obtain more efficient energy consumption.

© 2022 The Authors. Published by Universitas Muhammadiyah Malang
This is an open access article under the CC BY SA license. (https://creativecommons.org/licenses/by-sa/4.0/)

2. Research Method

As a benchmark for our proposed energy consumption model, this study creates a network structure for the EAM-LoRaNet. This section explains the structure and model.

2.1 Network Structure

The Nodes are distributed in EAM-LoRaNet in some rings that have a defined distance between them, forming a tree-based network as shown in Figure 1.

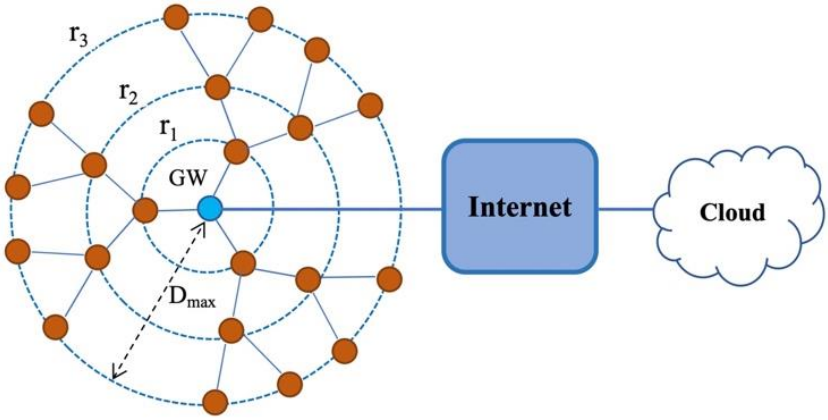

Figure 1. Structure Example of EAM-LoRaNet for IoT, Net = (R_g = 3, B_r = 3, C_h = 21)

The structure is made up of four parameters, which are as follows [11]:

- Number of Rings (R_g): the EAM-LoRaNet topology is made up of six rings. Each ring (r) has several nodes that are exactly positioned with the GW.
- Number of Branches (B_r): a branch connects GW to a node in the first ring directly. As a result, the number of branches in the first ring equals the number of nodes. A branch is changed to use a different channel to avoid packet collisions. As a result, the maximum number of channels is equal to the total number of channels. Because the maximum number of channels available for one sub-band with 61 Hz increments is eight, the number of branches is limited to eight.
- Several of node's children (C_h): each node has several offspring, with the exception of the nodes in the last ring (furthest ring).
- Maximum Distance (D_{max}) and Fixed Distance Between Rings (D_{ring}): the distance of the next ring is determined by the maximum distance that the highest transmission power P_{tx} and lowest receiver sensitivity S_{rx} can cover. The path loss formula yields Dmax, which is determined by Equation 1 [27]:

$$PL = 40\,(1 - 0.004H|_m)log_{10}D|_{km} - 18log_{10}H|_m + 21log_{10}f|_{MHz} + 80 \quad (1)$$

where:

H is the antenna height in meters
D is the distance of a node from GW in kilometers
f is the carrier frequency in MHz

If the antenna height H = 2 meters, the path loss of Equation 1 can be simplified to following Equation 2.

$$PL = 74.58 + 39.68\,log_{10}D|_{km} + 21log_{10}f|_{MHz} \quad (2)$$

The fixed distance spreading between rings is given by the proportion D_{max}/R_g, i.e. $d(r) = r(D_{max}/R_g)$. As a result, using Equation 3, the number of nodes in the EAM-LoRaNet may be determined based on the number of nodes in each branch and ring [28].

$$N_n = B_r \sum_{r=1}^{R_g} C_h^{r-1} \quad (3)$$

2.2 Energy Consumption Model

LoRa is a low-power wide-area network (LPWAN) technology that runs on a single battery and can last for years. Therefore, energy usage must be taken into account when operating the Lora. In order to extend the network lifetime, we discuss the energy consumption model for single-hop and multi-hop uplink transmission models in this section.

Each node in a ring sends its packet directly to the gateway in the single-hop uplink transmission, therefore it does not receive packets from any other node in the network to be sent to the gateway. As a result, the single-hop uplink's overall energy usage is the sum of three states: sending, sleeping, and idle. Thus, Equation 4 can be used to compute total energy consumption.

$$e_{tot} = e_{tx} + e_{sleep} + e_{idle} \tag{4}$$

The set of nodes in each ring plays two roles in the multi-hop uplink transmission scheme. The packet is only sent straight to the gateway by the nodes in the furthest ring. In the meantime, the nodes in the other rings (save the farthest ring) receive and transmit the packets to the gateway. As a result, the total energy consumption of the set of nodes at the farthest ring is identical to that of the single-hop uplink model using the equation (3). The set of nodes in the other rings, on the other hand, spend the energy that is equal to the sum of the energy consumed in transmitting, receiving, sleeping, and idle states. As a result, Equation 5 can be used to calculate total energy consumption.

$$e_{tot} = e_{tx} + e_{rx} + e_{sleep} + e_{idle} \tag{5}$$

We devise an algorithm in each node to calculate the overall energy usage for both uplink transmission methods. The energy consumption for each of the node's four states can be calculated using this approach. Thus, the total energy (e_{tot}) in line 13 will always increase based on the current state of the node. The difference time between the current simulation and the last update time is used to calculate the duration of the idle and sleep states (lines 5 and 7). Meanwhile, the Time on Air (ToA) of the packet, which is determined using Equations 6 to Equation 9, is used to determine the duration of the packet transmission (T_{packet}) (lines 9 and 11).

Algorithm Calculating the total energy consumption

Input: idle current: I_{idle}; sleep current: I_{sleep}; tx current: I_{tx}; rx current: I_{rx}; packet duration: T_{packet}; current state: *cs*
Output: total energy consumption: e_{tot}

1: $e_{cs} \leftarrow 0$ (energy consumption for the current state)
2: $V_D \leftarrow 3.3$ (supply voltage in volt)
3: **switch** *cs* **do**
4: **case**: IDLE
5: $e_{cs} = duration.GetSecond * I_{idle} * V_D$
6: **case**: SLEEP
7: $e_{cs} = duration.GetSecond * I_{sleep} * V_D$
8: **case**: TX
9: $e_{sc} = T_{packet} * I_{tx} * V_D$
10: **case**: RX
11: $e_{sc} = T_{packet} * I_{rx} * V_D$
12: **endSwitch**
13: $e_{tot} += e_{cs}$

The Time on Air (ToA) of the packet is [29].

$$T_{packet} = T_{preamble} + \eta_{pldSym} + T_{sym} \tag{6}$$

Where the preamble duration, symbol duration, and the number of payload and header symbols are represented in Equations 7, Equation 8, and Equation 9 respectively [29].

$$T_{preamble} = (\eta_{preamble} + 4.25) * T_{sym} \tag{7}$$

$$T_{sym} = \frac{2^{SF}}{BW} \tag{8}$$

© 2022 The Authors. Published by Universitas Muhammadiyah Malang
This is an open access article under the CC BY SA license. (https://creativecommons.org/licenses/by-sa/4.0/)

$$\eta_{pldSym} = 8 + \max(ceil(\frac{8PS - 4SF + 28 + 16 - 20H}{4(SF - 2DE)})(CR + 4), 0) \quad (9)$$

Where PS is payload size, SF is spreading factor, H is header mode setting (implicit mode = 1 and explicit mode = 0), DE is low rate optimization setting (DE = 1 for enable, and DE = 0 for disable), and CR is coding rate (valuable 1 to 4).

A LoRa packet's header mode can be implicit or explicit [29]. The number of symbols in the packet is determined by the LoRa packet formatting, as shown in Equation 9. When the header enable (H) value is set to 1, the implicit mode is selected. The idle current (I_{idle}), sleep current (I_{sleep}), and rx current (I_{rx}) (lines 5, 7 and 11) respectively are assigned based on the datasheet of SX1276 LoRa Transceiver [29]. Furthermore, the tx cur rent is obtained from the transmission power divided by the supply voltage ($P_{tx}|_{Watt}/(V_D|_{Volt} * \theta$), in which the transmission power is converted from dBm into Watt.

3. Results and Discussion

In this study, performance evaluation refers to the process of analyzing the impact of the transmission model on energy consumption and network longevity. The performance of the EAM-LoRaNet was analyzed using a network simulator NS-3 version 3 that includes basic LoRaWAN modules developed by [10]. In addition, the fundamental modules were extended to suit the needs of the LoRa transmission model in single-hop and multi-hop modes. The transmission current model, propagation model, and radio energy model are among the enhanced modules. We built two modules to replicate both single-hop and multi-hop uplink transmission.

3.1 Simulation Scenario

The configurations of LoRa packet structure, network structure parameters, and transmission configuration for single-hop and multi-hop are all taken into account in this simulation. As stated in Table 1, in this study, the LoRa packet structure uses the implicit model with the Header and Cyclic Redundancy Check (CRC) disabled. Table 2 shows the network structure, which comprises two scenarios using the SX1276 Lora transceiver model. The LoRa transceiver model, node's initial energy of joule, number of rings, number of branches, and number of children in each branch are all required setup parameters for the EAM-LoRaNet network structure as shown in Figure 1.

Table 1. Configuration of LoRa Packet Structure

Parameter	Value
Bandwidth (BW)	125 kbps
Uplink Frequency	915MHz
Coding Rate (CR)	1
Number of Preamble Symbols	8
Header Disable	0
Cycle Redundancy Check (CRC) Enable	0
Low Date Rate Optimization Enable	0

Table 2. Network Structure Parameter

Parameter	Scenario 1	Scenario 2
Initial Energy	2.5 Joule	2.5 Joule
Number of rings (Rg)	6	6
Number of branches (Br)	2	3
Number of children (Ch)	2	2
Number of nodes (N)	126	189

3.2 Experimental Results

Three performance evaluations of the single-hop and multi-hop models are used in this investigation. The first is a comparison of the single-hop and multi-hop ring's energy consumption, the second is an evaluation of increasing the spreading factor by one against energy consumption, and the third is a measurement of the number of periods and the amount of energy consumption of the network in the bottleneck.

3.2.1 Ring's Energy Consumption

The first experiment compares the ring's energy consumption for single-hop and multi-hop models, using scenario 1. Even though this experiment only examines a condition from scenario 1, it can represent all conditions from both

scenarios because it has the same characteristic for all of them. The energy consumed by a node in each ring of the network is shown in this experiment for both single-hop and multi-hop models. Figure 2 demonstrates that each node in the single-first hop's ring (closest ring) spends more energy than each node in the sixth ring (farthest ring), where the energy consumed is the total of energy spent transmitting, sleeping, and standing by. The first ring, the nearest ring, requires just 7 dBm of transmission power to send a packet to the GW, whereas the further ring requires 20 dBm of transmission power to send a packet straight to the GW. Figure 3 depicts the multi-hop energy consumption, which includes total energy (e_{tot}), transmitting-state energy (e_{tx}), and receiving-state energy (e_{rx}). The sum of energy used in transmitting, receiving, sleeping, and standby is referred to as multi-hop consumption. As illustrated in Figure 3, e_{rx} appears to have no substantial influence on the total energy increase, even though the nodes at each ring (except the farthest ring) conduct packet aggregation to be transmitted to the nodes at the GW's next-closer ring. Although receiving-state energy is added, the overall energy of the multi-hop is lower than that of the single-hop. As a result, compared to the single-hop model, the multi-hop model uses less energy.

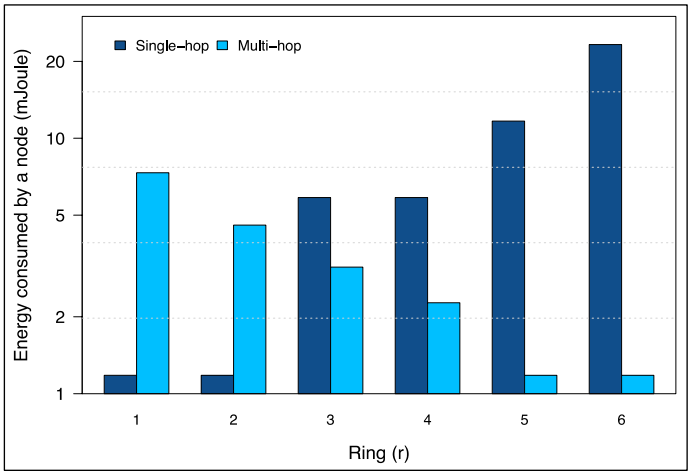

Figure 2. Energy Consumed by a Node in Each Ring for Single-hop and Multi-hop

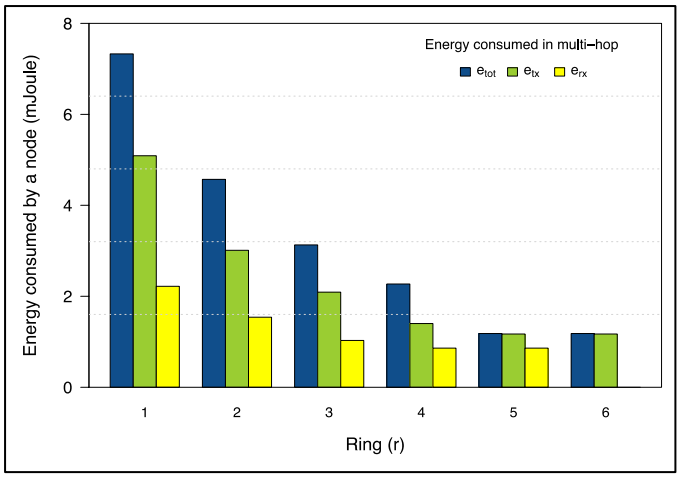

Figure 3. Energy Consumed by a Node in Each Ring for e_{tot}, e_{tx} and e_{rx} in Multi-hop

3.2.2 Spreading Factor Effect

Using scenario 1, the second experiment evaluates the effect of raising the spreading factor by one on energy consumption. The impact of increasing the SF by one versus increasing the energy consumption in each ring for single-hop and multi-hop models can be shown in Figure 4(a) and 4(b). The increase in SF by one in the first model is accompanied by a large increase in energy consumption in each node at each ring. In each ring, the greatest SF of 12 consumes more energy than the lowest SF of 7. The effect of increasing SF by one causes the Time on Air (ToA) to increase, resulting in an increase in energy consumption, where energy consumption is multiplied by ToA and transmission power. Furthermore, it appears that the outermost ring consumes more energy than the innermost ring. It occurs because the ring, in order to transmit packets straight to the GW, requires the highest transmission power of 20 dBm. The multi-hop model, on the other hand, is similar to the single-hop model in that it increases the SF by one,

© 2022 The Authors. Published by Universitas Muhammadiyah Malang
This is an open access article under the CC BY SA license. (https://creativecommons.org/licenses/by-sa/4.0/)

causing each ring to consume more energy. However, it grows at a slower rate than the single-hop. The cause is that nodes in each ring deliver packets to the next ring in one hop utilizing the lowest transmission power of seven dBm. Furthermore, as the node root of their branch, the nodes spend the most energy in the closest ring. Clearly, the multi-hop model consumes less energy than the single-hop model in each ring and across the entire network.

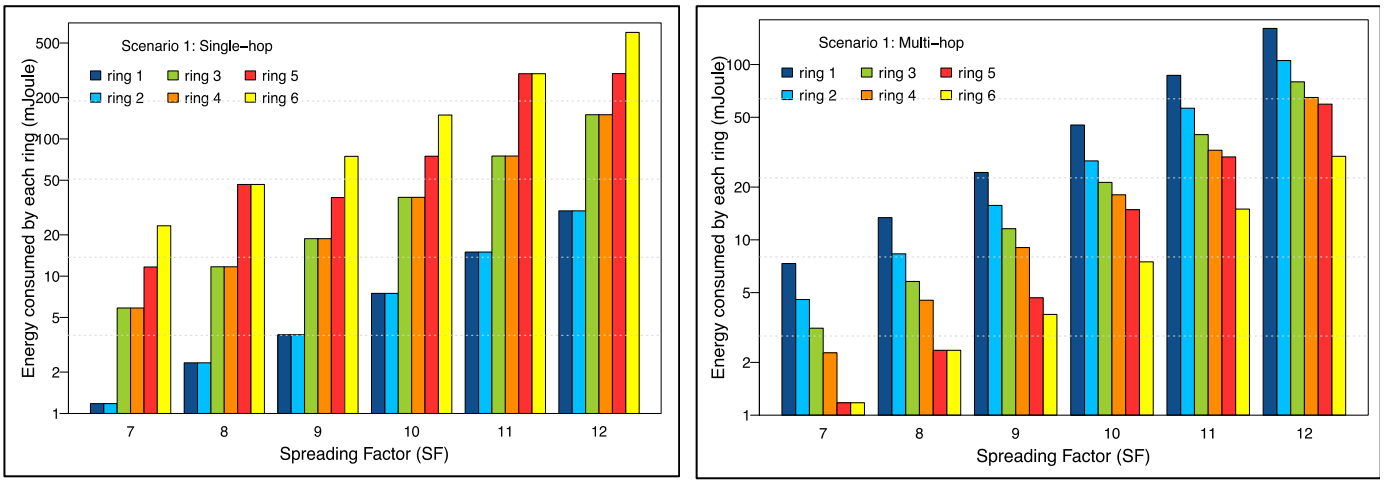

(a) Single-hop (b) Multi-hop

Figure 4. The Energy Consumed by Each Ring in the Network in Scenario 1 for Single-hop and Multi-hop

3.2.3 Network in a Bottleneck

In the third experiment, we measure the network bottleneck using two scenarios. The bottleneck is measured using two performance parameters: the consumption of the bottleneck and the number of periods. The amount of energy consumed by the network until it becomes a bottleneck is referred to as the bottleneck's consumption. Whiles, the number of periods refers to the number of times each node in a ring successfully conducts data sensing, gathering, and delivering packets to the GW before their energy is depleted. As we know, the single-hop's bottleneck occurs in the last ring (furthest ring), while the multi-hop's bottleneck occurs in the first ring (closest ring).

The total energy that spent by all nodes in the network for scenarios 1 and 2 is shown in Figure 5(a) and 5(b). In both instances, the multi-hop consumes significantly less energy than the single-hop. Figure 6(a) and 6(b) illustrate that the multi-hop has a greater number of periods than the single-hop. With all assigned spreading factor settings, both performance parameters appear in both cases. Furthermore, in the multi-hop, the number of periods decreases dramatically while the spreading factor increases by one. Meanwhile, there is a decrease in the number of periods in single-hop, although it is not as dramatic as in multi-hop. Clearly, the multi-hop network consumes far less energy and has a significantly longer network lifetime than single-hop networks.

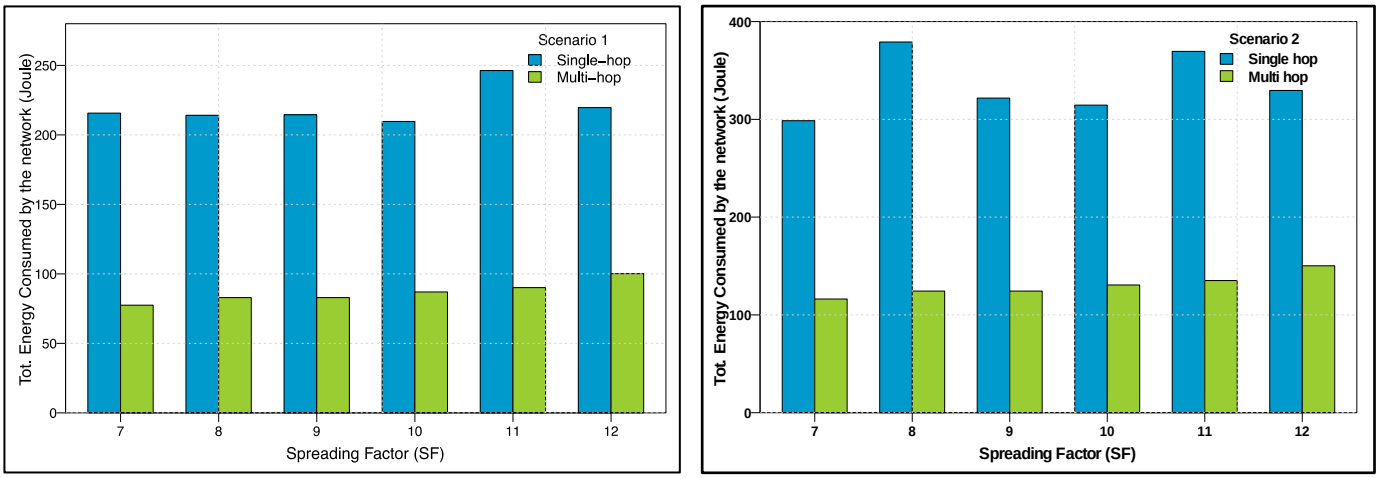

(a) Scenario 1 (b) Scenario 2

Figure 5. Network's Total Energy Consumption of Scenario 1 and Scenario 2

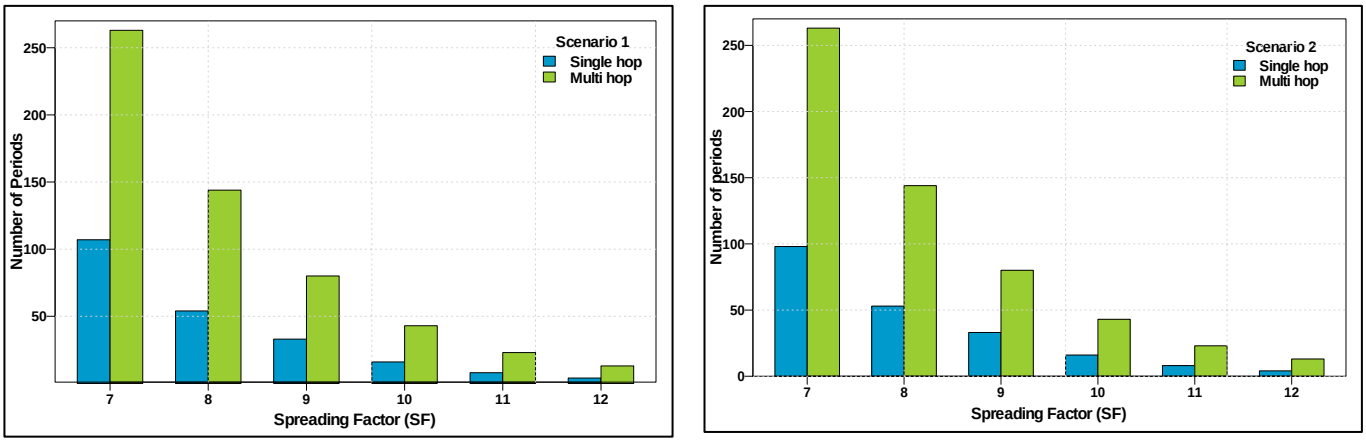

(a) Scenario 1 (b) Scenario 2

Figure 6. The Number of Periods until a Reached Bottleneck in Scenario 1 and 2 for Single-hop and Multi-hop.

4. Conclusion

The Energy Aware Multi-Hop LoRa Network (EAM-LoRaNet) was developed in this paper as a multi-hop uplink paradigm for LoRa Networks. The network performance was measured in terms of energy savings and network lifetime. The simulation findings reveal that a node in each ring consumes less energy in the multi-hop model than in the single-hop model. As a result, the multi-total hop's energy is lower than the single-hop's. While the influence of the spreading factor in the network revealed that the multi-hop model consumed less energy than the single-hop model in both each ring and the entire network. Finally, for the network lifetime that was assessed based on the network under bottleneck situation, the multi-hop had a longer network lifetime than the single-hop. Multi-hop models, in average, have better network performance in terms of energy savings than single-hop models.

Acknowledgment

We would like to express our gratitude to the University of Mataram for funding this research through the DIPA BLU capacity building scheme (contract number: 2927/UI18.L1/PP/2021).

References

[1] C. Kuhlins, B. Rathonyi, A. Zaidi, and M. Hogan, "Cellular Networks for Massive IoT, Ericsson White paper," 2020.
[2] A. J. Jara, A. F. Alcolea, M. A. Zamora, and A. F. G. Skarmeta, "Analysis of different techniques to define metadata structure in NFC/RFID cards to reduce access latency, optimize capacity, and guarantee integrity," *IFAC Proc. Vol.*, vol. 43, no. 4, pp. 192–197, 2010. https://doi.org/10.3182/20100701-2-PT-4011.00034
[3] E. Park, M.-S. Lee, H.-S. Kim, and S. Bahk, "AdaptaBLE: Adaptive control of data rate, transmission power, and connection interval in bluetooth low energy," *Comput. Networks*, vol. 181, p. 107520, 2020. https://doi.org/10.1016/j.comnet.2020.107520
[4] T. Benmansour, T. Ahmed, S. Moussaoui, and Z. Doukha, "Performance analyses of the IEEE 802.15.6 Wireless Body Area Network with heterogeneous traffic," *J. Netw. Comput. Appl.*, vol. 163, p. 102651, 2020. https://doi.org/10.1016/j.jnca.2020.102651
[5] L. Tian, S. Santi, A. Seferagić, J. Lan, and J. Famaey, "Wi-Fi HaLow for the Internet of Things: An up-to-date survey on IEEE 802.11ah research," *J. Netw. Comput. Appl.*, vol. 182, p. 103036, 2021. https://doi.org/10.1016/j.jnca.2021.103036
[6] X. Chen, Y. Xiao, Y. Cai, J. Lu, and Z. Zhou, "An energy diffserv and application-aware MAC scheduling for VBR streaming video in the IEEE 802.15.3 high-rate wireless personal area networks," *Comput. Commun.*, vol. 29, no. 17, pp. 3516–3526, 2006. https://doi.org/10.1016/j.comcom.2006.01.020
[7] Ompal, V. M. Mishra, and A. Kumar, "FPGA Integrated IEEE 802.15.4 ZigBee Wireless Sensor Nodes Performance for Industrial Plant Monitoring and Automation," *Nucl. Eng. Technol.*, 2022. https://doi.org/10.1016/j.net.2022.01.011
[8] G. Knieps and J. M. Bauer, "Internet of things and the economics of 5G-based local industrial networks," *Telecomm. Policy*, p. 102261, 2021. https://doi.org/10.1016/j.telpol.2021.102261
[9] D. Zorbas, K. Abdelfadeel, P. Kotzanikolaou, and D. Pesch, "TS-LoRa: Time-slotted LoRaWAN for the Industrial Internet of Things," *Comput. Commun.*, vol. 153, pp. 1–10, 2020. https://doi.org/10.1016/j.comcom.2020.01.056
[10] R. Islam, M. W. Rahman, R. Rubaiat, M. M. Hasan, M. M. Reza, and M. M. Rahman, "LoRa and server-based home automation using the internet of things (IoT)," *J. King Saud Univ. - Comput. Inf. Sci.*, 2021. https://doi.org/10.1016/j.jksuci.2020.12.020
[11] P. Boccadoro, V. Daniele, P. Di Gennaro, D. Lofù, and P. Tedeschi, "Water quality prediction on a Sigfox-compliant IoT device: The road ahead of WaterS," *Ad Hoc Networks*, vol. 126, p. 102749, 2022. https://doi.org/10.1016/j.adhoc.2021.102749
[12] R. K. Jha, Puja, H. Kour, M. Kumar, and S. Jain, "Layer based security in Narrow Band Internet of Things (NB-IoT)," *Comput. Networks*, vol. 185, p. 107592, 2021. https://doi.org/10.1016/j.comnet.2020.107592
[13] W. Ayoub, A. E. Samhat, F. Nouvel, M. Mroue, H. Jradi, and J.-C. Prévotet, "Media independent solution for mobility management in heterogeneous LPWAN technologies," *Comput. Networks*, vol. 182, p. 107423, 2020. https://doi.org/10.1016/j.comnet.2020.107423
[14] S. Farrell, *Low-Power Wide Area Network (LPWAN) Overview*. Internet Engineering Task Force (IETF), 2018.
[15] M. E. Yuksel and H. Fidan, "Energy-aware system design for batteryless LPWAN devices in IoT applications," *Ad Hoc Networks*, vol. 122, p. 102625, 2021. https://doi.org/10.1016/j.adhoc.2021.102625
[16] M. Bor, J. E. Vidler, and U. Roedig, "LoRa for the Internet of Things," in *International Conference on Embedded Wireless Systems and Networks (EWSN) 2016*, 2016, pp. 361–366.

© 2022 The Authors. Published by Universitas Muhammadiyah Malang
This is an open access article under the CC BY SA license. (https://creativecommons.org/licenses/by-sa/4.0/)

[17] C.-H. Liao, G. Zhu, D. Kuwabara, M. Suzuki, and H. Morikawa, "Multi-Hop LoRa Networks Enabled by Concurrent Transmission," *IEEE Access*, vol. 5, pp. 21430–21446, 2017. https://doi.org/10.1109/ACCESS.2017.2755858
[18] H.-C. Lee and K.-H. Ke, "Monitoring of Large-Area IoT Sensors Using a LoRa Wireless Mesh Network System: Design and Evaluation," *IEEE Trans. Instrum. Meas.*, vol. 67, no. 9, pp. 2177–2187, 2018. https://doi.org/10.1109/TIM.2018.2814082
[19] D. Lundell, A. Hedberg, C. Nyberg, and E. Fitzgerald, "A Routing Protocol for LoRA Mesh Networks," in *19th IEEE International Symposium on a World of Wireless, Mobile and Multimedia Networks, WoWMoM 2018*, 2018. https://doi.org/10.1109/WoWMoM.2018.8449743
[20] J. Dias and A. Grilo, "Multi-hop LoRaWAN uplink extension: specification and prototype implementation," *J. Ambient Intell. Humaniz. Comput.*, vol. 11, no. 3, pp. 945–959, 2020. https://doi.org/10.1007/s12652-019-01207-3
[21] A. Abrardo and A. Pozzebon, "A multi-hop lora linear sensor network for the monitoring of underground environments: The case of the medieval aqueducts in Siena, Italy," *Sensors (Switzerland)*, vol. 19, no. 2, 2019. https://doi.org/10.3390/s19020402
[22] C. T. Duong and M. K. Kim, "Reliable multi-hop linear network based on LoRa," *Int. J. Control Autom*, vol. 11, pp. 143–154, 2018. https://doi.org/10.14257/ijca.2018.11.4.13
[23] G. Zhu, C.-H. Liao, T. Sakdejayont, I.-W. Lai, Y. Narusue, and H. Morikawa, "Improving the Capacity of a Mesh LoRa Network by Spreading-Factor-Based Network Clustering," *IEEE Access*, vol. 7, pp. 21584–21596, 2019. https://doi.org/10.1109/ACCESS.2019.2898239
[24] D. L. Mai and M. K. Kim, "Multi-hop lora network with pipelined transmission capability," *Lect. Notes Comput. Sci. (including Subser. Lect. Notes Artif. Intell. Lect. Notes Bioinformatics)*, vol. 12293, pp. 125–135, 2020. https://doi.org/10.1007/978-3-030-58008-7_10
[25] D. L. Mai and M. K. Kim, "Multi-hop LoRa network protocol with minimized latency," *Energies*, vol. 16, no. 3, 2020. https://doi.org/10.3390/en13061368
[26] C. Ebi, F. Schaltegger, A. Rust, and F. Blumensaat, "Synchronous LoRa Mesh Network to Monitor Processes in Underground Infrastructure," *IEEE Access*, vol. 7, pp. 57663–57677, 2019. https://doi.org/10.1109/ACCESS.2019.2913985
[27] 3GPP, "3rd Generation Partnership Project; Technical Specification Group Radio Access Network; Evolved Universal Terrestrial Radio Access (E-UTRA); Radio Frequency (RF) system scenarios (Release 13)," 36.942, 2016.
[28] S. Barrachina-Muñoz, B. Bellalta, T. Adame, and A. Bel, "Multi-hop communication in the uplink for LPWANs," *Comput. Networks*, vol. 123, pp. 153–168, Aug. 2017. https://doi.org/10.1016/J.COMNET.2017.05.020
[29] S. Corporation, "SX1276/77/78/79 - 137 MHz to 1020 MHz Low Power Long Range Transceiver," 2019.

© 2022 The Authors. Published by Universitas Muhammadiyah Malang
This is an open access article under the CC BY SA license. (https://creativecommons.org/licenses/by-sa/4.0/)